

Bright galaxies from WENSS

I. The minisurvey*

H.R. de Ruiter^{1,2}, P. Parma², G.M. Stirpe¹, I. Perez-Fournon³, I. Gonzalez-Serrano⁴,
R.B. Rengelink⁵, and M.N. Bremer⁶

¹ Osservatorio Astronomico di Bologna, Via Zamboni, 33, I-40126 Bologna, Italy

² Istituto di Radioastronomia del CNR, Via Gobetti, 101, I-40129 Bologna, Italy

³ Instituto de Astrofísica de Canarias, E-38200 La Laguna, Tenerife, Spain

⁴ Instituto de Física de Cantabria, Universidad de Cantabria, Avda. de los Castros, E-39005 Santander, Spain

⁵ Leiden Observatory, P.O. Box 9513, 2300 RA, Leiden, The Netherlands

⁶ Institut d'Astrophysique de Paris, 98 bis Boulevard Arago, F-75014 Paris, France

Received 28 April 1998 / Accepted 17 July 1998

Abstract. A search for bright galaxies associated with radio sources from the WENSS minisurvey has been carried out. A galaxy counterpart was found for 402 of almost 10,000 radio sources. Of these a radio and optically complete sample, with a flux density limit at 325 MHz of 30 mJy and a limiting red magnitude of 16, can be constructed, which contains 119 galaxies.

This paper is the first step of a more general study, in which we aim to derive a bright galaxy sample from the entire WENSS survey (which is now available in the public domain) and thus to construct practically definitive local radio luminosity functions of elliptical and spiral galaxies.

We briefly describe the WENSS minisurvey, and the steps that are needed for the optical identification of its radio sources. Due to the large numbers of sources involved (over 200,000) completely automated procedures are obviously needed and we discuss these in some detail. It is shown that with modern utilities projects as described here have become quite feasible.

Some results (e.g. a preliminary determination of the local radio luminosity function) are presented.

Key words: galaxies: distances and redshifts — radio continuum: galaxies

1. Introduction

New radio source surveys covering large parts of the sky down to low flux densities are now rapidly becoming available. The NRAO VLA Sky Survey (NVSS) and Faint Images of the Radio Sky (FIRST) are both at 20 cm, but with different resolutions (Condon et al. 1998, Becker et al. 1995), and contain hundreds of thousands to several million radio sources. A parallel survey, at

92 cm, has been carried out with the Westerbork Radio Synthesis Telescope (WSRT) and is similar in size to the VLA surveys (Rengelink et al. 1997). Moreover, the Westerbork Northern Sky Survey (WENSS) has a resolution (of order one arcminute) similar to the NVSS.

It is clear that these new surveys will start a whole new chapter in the field of extragalactic research. The fact that the surveys are done at different frequencies will make it possible to study large numbers of sources with extreme spectra, like ultra-steep spectrum, peaked spectrum, and flat spectrum sources (the latter often being high-redshift quasars); it also allows us to do systematic searches for very rare events like gravitational lenses (see the CLASS project, Myers et al. 1995). Moreover, “classical” topics can now be studied in unprecedented detail. Optical/Infrared identification of radio sources can lead to very big complete samples of quasars and galaxies (both ellipticals and spirals), over a much wider range of intrinsic properties, such as radio power, than has hitherto been possible.

Although the observations of WENSS have now been completed, a subsample (the WENSS minisurvey) is in an advanced state of analysis (see Rengelink et al. 1997). Moreover, the minisurvey was crosscorrelated with optical data, resulting in a sample of “bright” ($m_r < 16.5$) galaxy identifications. We report on this sample of galaxy identifications in the present paper.

A very brief description of the minisurvey of WENSS is given in Sect. 2; the construction of a sample of galaxies associated with minisurvey sources is discussed in Sect. 3. Although many galaxies have known redshifts (because they are bright) this is by no means true for all galaxies in the sample. We therefore started a program of optical spectroscopy, the first results of which are discussed in Sect. 4. Another readily available property is the radio spectral index between 325 MHz (the observing frequency of WENSS) and 1400 MHz (the observing frequency of the NVSS, which also has a very similar angular resolution); this is discussed in Sect. 5. Some first results, like a determination of the local radio luminosity functions of ellipticals and

Send offprint requests to: H.R. de Ruiter

* Table 1 is only available in electronic form at the CDS via anonymous ftp to cdsarc.u-strasbg.fr (130.79.128.5) or via <http://cdsweb.u-strasbg.fr/Abstract.html>

spirals, are given in Sect. 6, while an outline of future related work is described in Sect. 7.

2. The WENSS minisurvey

The minisurvey (Rengelink et al. 1997) is a region of about 541 square degrees, at the North Ecliptic Pole. A subregion of the minisurvey, covering about 500 square degrees was chosen for a preliminary study of bright galaxy identifications, and will be followed up in the near future by a general study of the entire WENSS survey, which is now publicly available.

The restricted region of the minisurvey, used in the present paper, consists of two contiguous areas, with limits: right ascension between 15^{h} and 20^{h} , declination between 62° and $72^{\circ}30'$ for the first area, and $15^{\text{h}}30^{\text{m}}$ to 20^{h} , 57° to 62° for the second area. It contains 9810 radio sources (the entire minisurvey 11299). Of these 9810 sources 6931 have a peak flux density > 30 mJy; these will be used in the determination of the radio luminosity function, since WENSS is expected to be complete at that level (Rengelink et al. 1997). We refer to the paper of Rengelink et al. (1997) for further detailed information on the WENSS project, and the reduction procedures followed by them.

3. The galaxy identifications

3.1. Optical identification procedure

Generally the optical identification procedure is quite straightforward: an identification is considered to be positive if the radio and optical positions are within some adopted maximum distance, and for the whole identification sample the completeness and reliability can easily be established (see e.g. De Ruiter et al. 1977).

In the case of bright galaxies the usual criteria have to be applied with somewhat more caution, because many of the galaxies are extended, and in a few cases very extended (cf. NGC 6503 in Table 1). Therefore there is the risk of losing very bright galaxies if we only use a pre-established limit in the radio-optical separation (the radio source does not necessarily fall exactly on the optical center, in particular in the case of spiral or starburst galaxies). For this reason we started with a large search area with radius 30 arcsec around the radio position, and then decided on the basis of the extension of the galaxy if it could be accepted as the optical counterpart of the radio source. Basically this was done for galaxies with magnitude brighter than 14, while fainter galaxies were treated in the usual way.

Considering the large quantity of radio sources (the more so in the future when we will use the entire WENSS), the identification procedure has to be automatized as much as possible. We proceeded in several steps: first, we cross-correlated the minisurvey sources with the Automated Plate Machine (APM) catalog of POSS I objects (McMahon & Irwin 1992), using a search radius of 30 arcsec. Of this list of optical objects thus produced, we selected a subset of those that were classified by the APM as non-stellar in at least one color. At this point in the analysis we therefore eliminated objects of stellar appearance (quasars

for example), and are left with galaxies. Their nominal APM magnitudes were required to be brighter than 18.5 in the blue or brighter than 17 in the red. This resulted in a first, tentative, list of about 800 possible galaxy identifications. We then extracted small optical images for this subset, using the “jukebox” and the Digital Sky Survey (based on red POSS prints). We are developing software that can decide whether an extended object is present near the radio source position, determine its magnitude, and produce an automatic listing of proposed galaxy identifications. Thus the whole identification procedure would then be reduced to preparing a list of source positions, extracting corresponding DSS images and determine the presence of optical counterparts. However, for the moment we have used the subset of proposed galaxy identifications based on the APM, and inspected each individual field visually. Thus we checked the nature of the object (galaxy or star-like), and its distance from the radio position. Since the errors in the radio position are typically of the order of a 2–3 arcsec (see Rengelink et al. 1997), the initial search radius of 30 arcsec is usually far too big. Only very bright and therefore very extended galaxies may be associated with radio sources that are relatively far away (> 10 arcsec) from the galaxy center. Such bright galaxies are often spirals, in which we may detect giant HII regions in the outer parts of the galaxy. Considering this we tightened our criteria at this point, requiring that the radio/optical position difference should not be more than 5 arcsec, except for the brighter galaxies, where we decided on an individual basis if the radio source was likely to be associated with the galaxy.

The magnitudes were calibrated using i) stars of selected area 57 (Grueff, private communication) and ii) the galaxies observed photometrically by Sandage (1972), Sandage (1973). From i) we could calibrate the point source magnitude and from ii) the galaxy diameter, which together then give the galaxy magnitude. It is therefore quite feasible to obtain in an automated fashion galaxy magnitudes, by determining the central photographic density, a mean source diameter (e.g. through a gaussian fit) and the background density. The rms uncertainty thus obtained for the Sandage galaxies is ~ 0.3 mag.

Our final list of identifications contains 402 galaxies. This list is by no means complete, since the selection was done using APM magnitudes. We believe optical completeness is achieved at about $m_r = 16$. This point is further discussed in Sect. 3.2.

In Fig. 1 we show the difference between radio and optical positions (in α and δ separately). Relatively large positional differences (> 5 arcsec) occur only for the brighter galaxies (see the discussion in the previous paragraph).

A simple estimate of the reliability of our identifications is straightforward: assuming that there are roughly 30 galaxies per square degree down to a red magnitude of 16, and assuming an average search radius of 10 arcsec, we expect of the order of 7 spurious identifications, among the ~ 9000 minisurvey sources. The actual number of identifications with $m < 16$ in Table 1 is 185, and therefore the contamination rate should be around 4%. For fainter objects the search radius was actually smaller (close to 5 arcsec, see above), so that the higher density of background galaxies, down to $m_r = 17$, is almost entirely compensated by

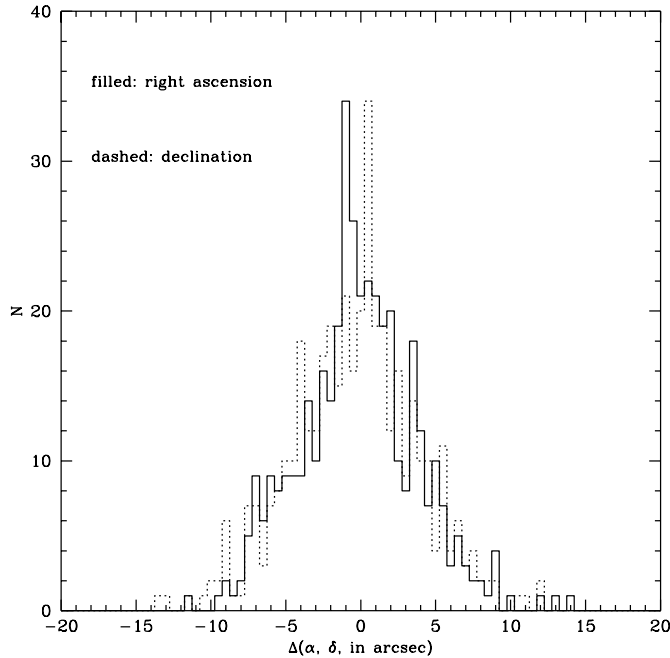


Fig. 1. Differences (in arcsec) of radio and optical positions.

the tighter search criterion. The overall contamination of the sample given in Table 1 is therefore $\sim 5\%$, which is quite acceptable.

The completeness is much harder to estimate, since we used a first selection criterion based on APM magnitudes required to be brighter than 17 in the red. These magnitudes are accurate for stellar objects, but may be wrong by as much as ~ 1 magnitude for galaxies around $m_r \sim 15 - 16$, and more than that at the bright end. Fortunately, compared to the magnitudes as calibrated from the Digital Sky Survey, the APM tends to overestimate the brightness of objects. If we impose a limit of $m_r = 16$ we should therefore be statistically complete, although individual objects may erroneously have crept in or dropped out of the sample due to the photometric uncertainty of our magnitudes (approximately 0.4 mag.). We conclude that very few objects will be missing.

3.2. The galaxy sample

The sample of galaxy identifications is given in Table 1. The lay-out of this table is: a running number based on the minisurvey radio catalogue, ordered in right ascension, in column 1, the WENSS name in column 2, peak and integrated flux densities at 325 MHz (S_{325} peak and total respectively) in columns 3 and 4, galaxy name (if any) and type (elliptical or spiral) in columns 5 and 6, the red magnitude (as discussed above) and (galactocentric) redshift, if known, in columns 7 and 8. Redshifts with an asterisk are based on the new observations described in the next section. The differences (in arcsec) of the radio and optical positions (in the sense radio minus optical) in right ascension and declination are given in columns 9 and 10, and finally the spectral index between 325 MHz (from WENSS) and 1400 MHz

(from NVSS, see below) in column 11: only spectral indices of sources with a 325 MHz peak flux density above 100 mJy are shown, because total fluxes of fainter sources may be systematically underestimated (see Sect. 5).

Table 1 contains all 402 galaxies that were found using the above selection criteria and it does not represent in any sense a complete sample. However it is straightforward to construct a radio and optically complete sample, once we take into account the following points:

i) The WENSS survey lists radio sources down to a flux density of 15 mJy, but is essentially complete only above $S_{325}(\text{peak}) = 30$ mJy. There are 274 galaxy identifications in Table 1 with radio flux density above this limit.

ii) Galaxies were first selected on the basis of their blue and red APM magnitudes, which means that some galaxies have m_r (determined afterwards) in the range 17–18 mag. Obviously we cannot claim to be complete at that magnitude level. A safe limit appears to be $m_r = 16$; there are 119 galaxies brighter than 16 and with radio flux density above 30 mJy. This should be considered a radio and optically complete sample. We may have missed some very low surface brightness galaxies, which should have been included on the basis of their integrated magnitude: especially the spiral galaxies given in Table 1 have a wide range of mean surface brightness, and one or two are barely detected although they are so extended as to have an integrated magnitude brighter than the $m_r = 16$ limit. We assume that such objects are rare and therefore only marginally affect the completeness of the sample.

In Fig. 2 we give the distribution of radio flux densities at 325 MHz of the galaxy identifications given in Table 1. The contribution of spiral galaxies in the histogram is represented by the shaded area. As is well known, spiral galaxies are mainly found below ~ 100 mJy, reflecting the fact that they are on average much weaker radio emitters than elliptical galaxies.

4. Optical spectroscopy

In 1995 international time was allocated at La Palma Observatory to the WENSS project, of which a small part was dedicated to bright galaxies. Here we report on the spectroscopic observations carried out with the Isaac Newton Telescope (INT). We used the R300V grating, covering the range 3800–7200 Å, and a slit of 220 μm (corresponding to 1.19 arcsec). The observing log is given in Table 2, where in column 1 we list the running number as in column 1 of Table 1. The spectra were reduced with the help of the IRAF package. The redshift data, which for most objects were determined for the first time, are given in Table 3, where we also list the presence or absence of emission lines (usually $H\alpha$). NEL in column 5 stands for narrow emission lines (if $H\alpha$ is indicated no other emission lines like [OIII] $\lambda\lambda 4959, 5007$ were detected). Emission lines were predominantly found in spiral galaxies, but with a few exceptions: the elliptical galaxy Zwicky 338.014 has a Seyfert 1.5 type spectrum ($H\alpha$ and $H\beta$ have weak broad components), while $H\alpha$ in emission is also present in the elliptical Zwicky 337.030. Redshift information is virtually complete for spiral galaxies with

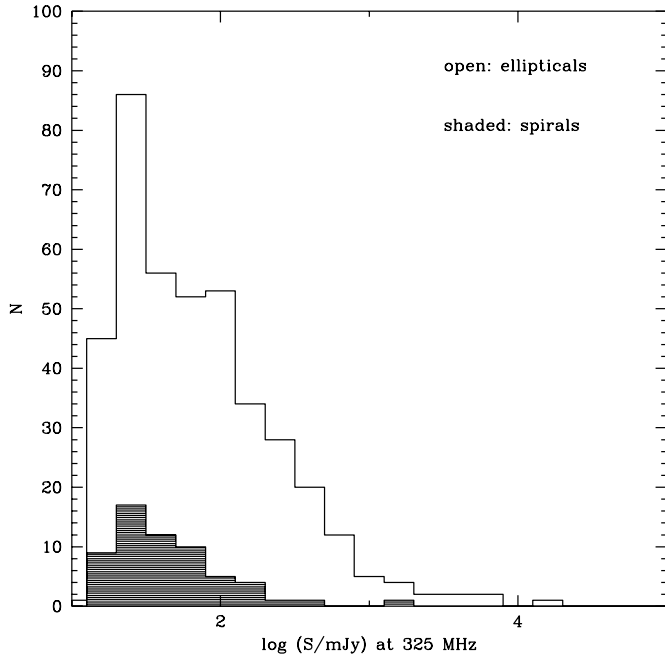


Fig. 2. Histogram of the flux density distribution of the galaxy identifications. The contribution of spirals is represented by the shaded area.

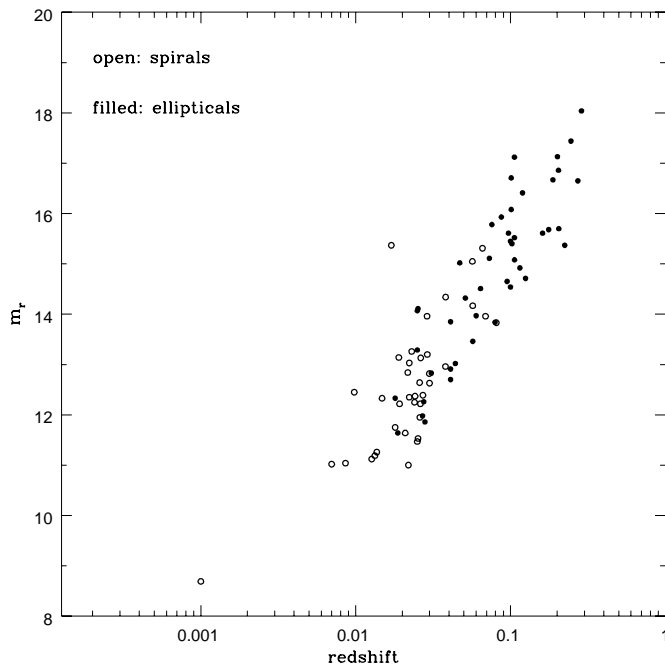


Fig. 3. redshift–magnitude relation for spirals and ellipticals with known redshift.

$m_r < 15$, but not for ellipticals ($\sim 20\%$ is still missing). A very modest effort will be needed in the near future to fill the gaps in redshift down to a red magnitude of 16. We give a Hubble diagram for those objects with known redshifts in Fig. 3.

Table 2. INT observing log

| Nr | Date yymmdd | UT | Exp. Time seconds |
|-------|----------------|-------|----------------------|
| 1758 | 950513 | 20:49 | 1200 |
| 1842 | 950512 | 21:33 | 1800 |
| 1941 | 950513 | 21:30 | 900 |
| 2441 | 950513 | 21:54 | 1200 |
| 2576 | 950511 | 00:46 | 1800 |
| 2761 | 950512 | 00:34 | 1800 |
| 2934 | 950513 | 22:22 | 1800 |
| 3148 | 950512 | 01:13 | 900 |
| 3734 | 950511 | 01:25 | 900 |
| 4570 | 950511 | 01:48 | 300 |
| 4604 | 950511 | 01:59 | 300 |
| 4744 | 950512 | 01:37 | 1200 |
| 4751 | 950511 | 02:12 | 900 |
| 4773 | 950513 | 23:17 | 1200 |
| 4933 | 950512 | 02:04 | 1800 |
| 5116 | 950513 | 23:44 | 900 |
| 5355 | 950511 | 02:35 | 300 |
| 6214 | 950513 | 00:46 | 1200 |
| 6234 | 950513 | 01:16 | 1200 |
| 6536 | 950511 | 02:47 | 300 |
| 6569 | 950511 | 02:57 | 300 |
| 7077 | 950511 | 03:11 | 1200 |
| 8572 | 950513 | 02:30 | 1800 |
| 8605 | 950511 | 03:53 | 600 |
| 8700 | 950512 | 03:49 | 900 |
| 8877 | 950513 | 03:09 | 1800 |
| 9377 | 950511 | 04:12 | 1200 |
| 9555 | 950513 | 03:54 | 1200 |
| 9582 | 950512 | 04:14 | 1200 |
| 9746 | 950513 | 04:23 | 1800 |
| 10687 | 950513 | 05:00 | 1200 |

5. Spectral indices

Now that both WENSS and NVSS are nearing completion it is fairly straightforward to derive spectral indices between 325 and 1400 MHz. It should be noted however that the NVSS gives *components*, obtained by doing Gaussian fits on the NVSS images. This means that different “sources” may refer to one and the same radio source, because they represent for example the core and the lobes separately. However, WENSS has already grouped such components into a radio source. Since the large quantities of data force us to use automatic procedures, we made a cross correlation with a deliberately large search radius of four arcmin, between the WENSS minisurvey sources and the NVSS. As a next step we then applied a source-dependent search radius, requiring that NVSS components should be considered as the 1400 MHz counterpart of the WENSS source only if i) the NVSS component was not more distant from the WENSS position than the WENSS beam size (taken as 54 arcsec), in the case of unresolved WENSS sources, ii) the NVSS component was closer than 1.5 times the largest angular size, in the case of resolved WENSS sources. This procedure reduces the contam-

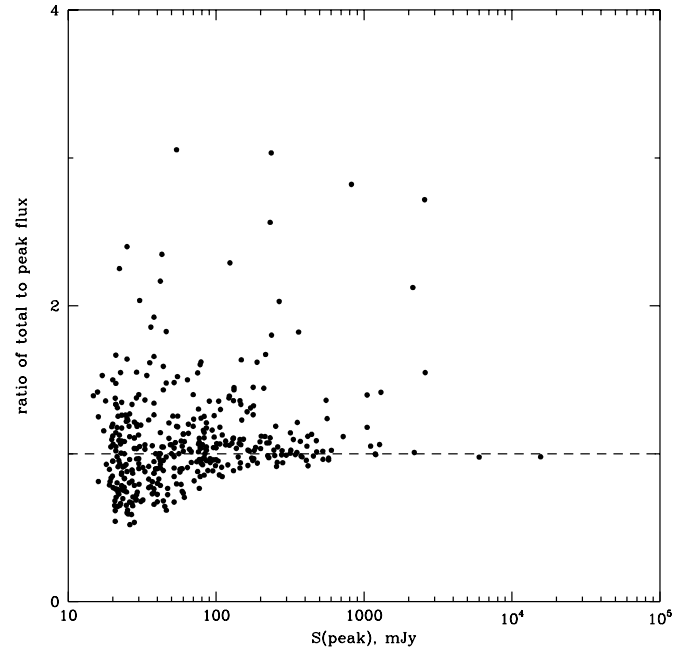
Table 3. Spectroscopic data

| Nr | Name | type | redshift | Comments |
|-------|--------------|------|----------|-----------------|
| 1758 | zw318.016 | S | 0.029 | NEL |
| 1842 | zw337.030 | E | 0.025 | NEL: H α |
| 1941 | | S | 0.023 | NEL |
| 2441 | | E | 0.115 | no EL |
| 2576 | | E | 0.101 | no EL |
| 2761 | | S | 0.057 | NEL |
| 2934 | zw338.014 | E | 0.025 | Seyf 1.5 |
| 3148 | ugc10072 | S | 0.025 | NEL |
| 3734 | | E | 0.125 | no EL |
| 4570 | ngc6214 | S | 0.026 | NEL: H α |
| 4604 | ngc6211 | E | 0.018 | no EL |
| 4744 | ugc10548 | S | 0.030 | NEL |
| 4751 | | S | 0.069 | NEL |
| 4773 | ugc10559 | S | 0.019 | NEL |
| 4933 | | E | 0.100 | no EL |
| 5116 | ngc6286 | S | 0.018 | NEL |
| 5355 | ngc6303 | E | 0.041 | no EL |
| 6214 | mcg12-16-046 | E | 0.060 | no EL |
| 6234 | zw340.008 | E | 0.041 | no EL |
| 6536 | ngc6457 | E | 0.027 | no EL |
| 6569 | ngc6463 | E | 0.041 | no EL |
| 7077 | zw340.028 | S | 0.081 | NEL |
| 8572 | | E | 0.106 | no EL |
| 8605 | | E | 0.102 | no EL |
| 8700 | ugc11363 | E | 0.044 | no EL |
| 8877 | ugc323.004 | S | 0.038 | NEL: H α |
| 9377 | | E | 0.095 | no EL |
| 9555 | | E | 0.073 | no EL |
| 9582 | | E | 0.100 | no EL |
| 9746 | | E | 0.097 | NEL |
| 10687 | | E | 0.064 | no EL |

ination of the 1400 MHz flux by unrelated background sources to a minimum, while at the same time guaranteeing the inclusion of most components (except perhaps for the very biggest sources).

There is one point which needs some more attention: in trying to derive radio spectral indices (using the NVSS) we should be careful that there are no, or only insignificant, hidden biases in the flux densities at 325 MHz and 1400 MHz. This is all the more important, as the enormous quantity of data forces one to follow automatic procedures. The routines used to derive integrated flux densities are slightly different in WENSS and NVSS: whereas NVSS makes gaussian fits of components, which are forced to give a source size that is at least as big as the beam, this is not so in WENSS, where the source size is directly related to the fit parameters (and these are allowed to be smaller than the beam). For strong sources the bias in spectral index should be so small as to be insignificant, but unfortunately for weaker sources ($S_{325}(peak) < 100$ mJy) this is not true, as is shown in Fig. 4.

WENSS tends to underestimate the integrated fluxes of the weak sources and we estimate that WENSS fluxes are on average

**Fig. 4.** Ratio of integrated to peak flux densities as a function of peak flux density, for identified radio sources.

too small by a factor of the order 10 % for sources with peak flux densities in the range $\sim 30 - 50$ mJy (see Fig. 4). An empirical correction factor Δ was determined, by which the integrated fluxes of Table 1 should be divided: $\Delta = 0.0768 \times (\log S_p)^2 - 0.228 \times \log S_p + 0.1315$, where S_p is the peak flux at 325 MHz in mJy. This correction is small above 100 mJy; it shifts the distribution of the ratio integrated/peak flux densities back to being symmetrical (in the logarithm) around unity, as we would expect if the scatter is purely due to the map noise. Of course, flux densities below 100 mJy should anyway be treated with caution.

For our galaxy identifications we find that the average spectral index between 325 and 1400 MHz is $\langle \alpha \rangle = 0.61 \pm 0.01$ (standard deviation of the mean). The spectral index distribution is shown in Fig. 5.

In particular the faintest sources (below 100 mJy) tend to have flat spectra, but we should keep in mind that we had to apply an empirical correction to the integral flux densities of WENSS, which may not have always succeeded in recovering the flux completely.

For WENSS sources with $S_{325} > 100$ mJy we have: $\langle \alpha \rangle = 0.66 \pm 0.03$.

This spectral index is significantly flatter than what is usually found for samples of radio sources. It is known, however, that the spectral index depends on radio power (Laing & Peacock 1980). Their correlation is mainly based on FR II sources, but it is most likely that the correlation extends down to the fainter end of the FR I sources (see Laing & Peacock 1980). In fact, if we take all minisurvey sources with $S_{325} > 100$ mJy (roughly 3100) and repeat the cross-correlation we get: $\langle \alpha \rangle = 0.82 \pm 0.01$. This is expected, as the bulk of the radio sources will be associated with

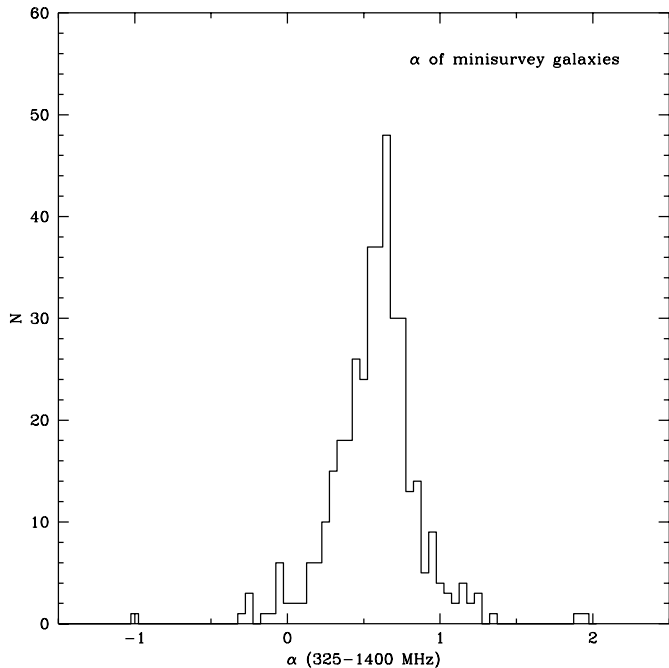


Fig. 5. Distribution of spectral index between 325 MHz (WENSS) and 1400 MHz (NVSS) for identified sources. Only very few WENSS sources were not covered by the NVSS.

quasars and galaxies of higher radio power, at larger distances than the sources of our nearby galaxy sample. We also checked that the spectral index of the galaxy sample was not significantly biased by resolution effects: since the sources are nearby they may have large angular diameters and consequently some flux may have been lost at 325 MHz. We therefore took only unresolved WENSS sources, for which we get a median $\alpha = 0.68$, or 0.67 if we exclude sources associated with spiral galaxies. This shows that any resolution effect is so small as to be insignificant. Using the relation between spectral index and power given by Laing & Peacock (1980), and assuming a median α of 0.67, our sample should consist of FR I radio galaxies peaked around a median power (at 325 MHz) of $\log P(WHz^{-1}) = 24.22$. The sample of elliptical galaxies given in Table 1 has a median $\log P(WHz^{-1}) = 24.00$ and is therefore entirely compatible with the Laing & Peacock relation.

6. Discussion and conclusions

The first thing that attracts attention is the large number of very bright and nearby galaxies associated with WENSS sources. Obviously, the new large-scale surveys will pick up large quantities of such nearby objects that were relatively scarce until now.

6.1. The identification content

For about 400 of the 9810 radio sources located in the restricted area of the minisurvey, used by us for identification purposes, a galaxy counterpart was found, with magnitude roughly brighter

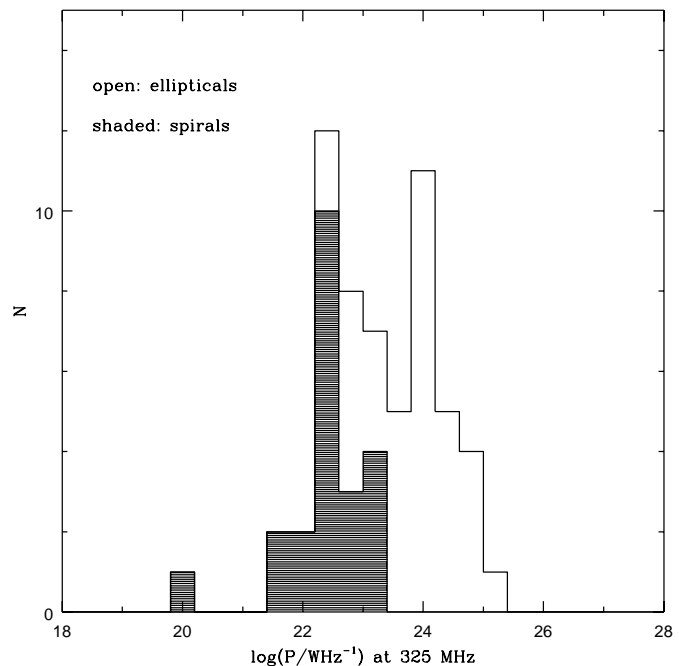


Fig. 6. Distribution of radio power at 325 MHz for galaxies of the minisurvey sample with $S_{325}(\text{peak}) > 100$ mJy and $m_r < 15$. The contribution of spirals is represented by the shaded area.

than 17–18 in the red (see Table 1). In Fig. 2 we show the distribution of flux densities over elliptical and spiral galaxies. As expected, spirals start to come in mainly below 100 mJy, reflecting the well known fact that spiral galaxies contain on average weaker radio sources than ellipticals. Using only objects with $S_{325} > 30$ mJy and $m_r < 15$, for which limit redshift information is essentially complete for spirals, we give in Fig. 6 the histogram of radio power. For ellipticals we assumed that, as a reasonable first approximation, their absolute magnitude can be considered constant (we took $M_r = -22.0$, for $H_0 = 100 \text{ km s}^{-1} \text{ Mpc}^{-1}$): redshifts are still missing for about a quarter of the ellipticals.

6.2. The radio luminosity functions

Although the majority of galaxies in Table 1 lacks redshift information, it is possible to make a first attempt to derive the radio luminosity function of starburst galaxies and AGNs, by limiting ourselves to sources with flux density $S_{325} > 30$ mJy (radio completeness limit) and to the optically bright tail: if we select only objects with $m_r < 15$ all spirals and most ellipticals ($\sim 75\%$) have redshift information. For the remaining ellipticals we assumed an absolute red magnitude of -22.0 (see above). If we use all galaxies, assuming a standard absolute magnitude for all spirals and ellipticals without z , we get $\langle V/V_m \rangle = 0.48 \pm 0.02$ for ellipticals and $\langle V/V_m \rangle = 0.30 \pm 0.03$ for spirals; therefore we may expect severe incompleteness of the spiral galaxy sample. However, with the limits $S_{325} = 30$ mJy, and $m_r = 15$ we get: $\langle V/V_m \rangle = 0.50 \pm 0.05$ (ellipticals) and $\langle V/V_m \rangle = 0.47 \pm 0.06$ (spirals), which sug-

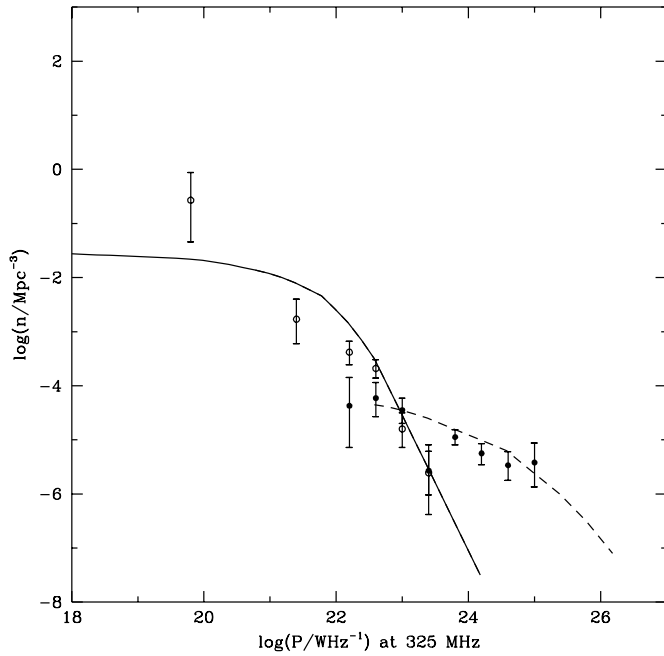


Fig. 7. The radio luminosity function of spiral and elliptical galaxies represented by open and filled circles respectively. For comparison we plot the RLF as derived by Condon (1989) for spirals (solid line) and ellipticals (dashed line).

gests that both categories of galaxies are essentially complete. The radio luminosity function thus calculated is shown in Fig. 7. For comparison we have also plotted the RLF of starforming galaxies and of AGNs as given by Condon (1989), shifted to 325 MHz, by using an average spectral index of 0.6. The qualitative agreement is evident. (Note that the high point at very low radio power is due to the detection of NGC 6503, a very bright and nearby galaxy.)

7. Future work

The present paper is the first in a series which will be dedicated to nearby galaxies associated with WENSS radio sources. Since the overall WENSS catalogue is a factor of roughly 20 larger than the minisurvey used here, we expect in the end to be able to study samples of roughly 8000 to 10000 bright galaxies. This should give us a unique opportunity to analyze various correlations (e.g. dividing the galaxy sample according to galaxy type, radio spectral index, angular size).

Acknowledgements. We thank the principal investigators of WENSS, Drs. George Miley and Ger de Bruyn, for their continual support, and Arno Schoenmakers for many helpful suggestions. We also thank Dr. Richard McMahon, who provided us with the APM data used in this paper and R. Primavera, who carried out astrometric measurements on the POSS prints. This work was partially supported by the European Commission, TMR programme, Research Network Contract ERBFMRXCT96-0034 “CERES”. The Isaac Newton Telescope is operated on the island of La Palma by the Royal Greenwich Observatory at the Spanish Observatorio del Roque de Los Muchachos of the Instituto de Astrofísica de Canarias. The Westerbork Synthesis Radio Telescope (WSRT) is operated by the Netherlands Foundation for

Research in Astronomy with financial support from the Netherlands Organisation for Scientific Research. The National Radio Astronomy Observatory is operated by Associated Universities, Inc., under contract with the National Science Foundation. This research has made use of the NASA/IPAC Extragalactic Database (NED) which is operated by the Jet Propulsion Laboratory, California Institute of Technology, under contract with the National Aeronautics and Space Administration. The 102 CDROM of the Digitized Sky Survey was produced at the Space Telescope Science Institute under U.S. Government grant NAG-W-2166.

References

- Becker R.H., White R.L., Helfand D.J., 1995, ApJ 450, 559
- Condon J.J., 1989, ApJ 338, 13
- Condon J.J., Cotton W.D., Greisen E.W., et al., 1998, AJ in press
- De Ruiter H.R., Arp H.C., Willis A.G., 1977, A&AS 28, 211
- Laing R.A., Peacock J.A., 1980, MNRAS 190, 903
- McMahon R.G., Irwin M.J., 1992, in: MacGillivray, H.T., Thomson, E.B. (eds.) Digitized Optical Sky Survey. Kluwer, Dordrecht, p. 417
- Myers S.T., Fassnacht C.D., Djorgovski S.G., et al., 1995, ApJ 447, L5
- Rengelink R.B., de Bruyn A.G., Miley G.K., et al., 1997, A&AS 124, 259
- Sandage A., 1972, ApJ 178, 25
- Sandage A., 1973, ApJ 183, 731